From Surfaces to Interfaces - Ambient Pressure XPS and beyond

Miquel Salmeron

Materials Sciences Division, Lawrence Berkeley National Laboratory, Berkeley, California 94720, United States
Department of Materials Science and Engineering, University of California, Berkeley, California 94720, United States

Introduction

The foundation for studies of surfaces with atomic level accuracy was laid down in the preceding decades by pioneers, starting with Irving Langmuir in the 1930's. The fastest advances however appeared in the decades following 1960, when vacuum technology made possible to prepare well characterized surfaces using single crystals in ultrahigh vacuum (UHV), describing a pressure regime well below 10^{-6} Torr, where the gas density is such that about 10^{15} molecules collide on 1 cm^2 per second. This number corresponds roughly to the density of surface atoms of most materials.

What we call today Surface Science techniques, including Auger-Meitner Electron Spectroscopy (AMES), Ion Scattering (IS), and X-ray based spectroscopies such as photoelectron emission (XPS), and particularly electron yield detection absorption spectroscopy (EY-XAS), were soon developed.[1] These techniques, which are inherently surface sensitive due to the short mean free path of electrons and ions, provide elemental identification of species present at surfaces within a depth of a few Angstrom, with a quantitative accuracy down to 1% of a monolayer or less. In addition these techniques provide also electronic information about the chemical state of the species. On the structural side, diffraction using low energy electrons (LEED), grazing angle of high energy electrons and X-rays (RHEED, GISAXS), and real space microscopies like Scanning Tunneling and Force Microscopies (STM, AFM), and Transmission Electron Microscopy (TEM) provided a rich set of tools that have allowed scientists to tackle the most fundamental problems and issues in Surface Science.

A limitation of the surface science approach is the difficulty of studying surfaces under realistic conditions of pressure and temperature close to those in human environments and in industrial catalytic processes. At ambient pressures optical techniques, like Raman, Infrared, Second Harmonic and Sum Frequency Generation

(SHG, SFG) spectroscopies provide a way to study surfaces from a vibrational spectroscopy point of view. Their surface sensitivity is dictated not by the penetration depth of light, but rather by selection rules for photon absorption and emission that affect species located at the surface. For techniques that are intrinsically surface sensitive, mostly based on electron and ion probes, the particles travel only a few atomic distances at energies of a few hundred eV electrons in condensed matter and a few mm in gases in the Torr pressure range, making their use very challenging. An exception to this are the STM and AFM proximal probes, because the tip used in these techniques to sense currents, forces, or to concentrate light via plasmon resonance with the tip apex, is always a few nanometers away from the surface, so that at only few gas or liquid species are present in the intervening space. The fundamental technical difficulties faced by AMES, and XPS were resolved in the early 2000's [3], thus enabling to bridge the pressure gap from UHV to ambient conditions. New acronyms for the modified techniques have been created by adding the words Ambient Pressure (AP) to the previous ones, thus creating APPES for ambient pressure photoelectron spectroscopy, or APXPS for ambient pressure XPS, often used indistinctly. Reviews of these techniques can be found in the literature [4], and will not be repeated here. In the present review we illustrate with a couple of APXPS results the scientific new research avenues made possible by their use. In the last part we discuss progress aimed at extending the range of "ambient pressure" to the atmospheric range and beyond, including dense environments such as liquid phases. We conclude with some remarks about problems that need to be resolved in the new burgeoning field of ambient pressure interface science.

In situ X-Ray spectroscopies reveal the initial step in the Fischer-Tropsch reaction

In the first example we how with the help of EY-XAS and APXPS the reaction pathways of CO and H_2 reaction in Fischer-Tropsch catalysis on cobalt could be clarified. To form hydrocarbons out of CO and H_2, a necessary step is the dissociation of CO. The molecular scale details of this process have been controversial for many years. The question is whether dissociation of CO molecules ($CO_{ads} \rightarrow C_{ads} + O_{ads}$) occurs directly, i.e., without assistance from other species or if, as proposed by theoretical calculations, other steps are involved, in particular if co-adsorbed H binds to CO to form H_nCO or

CH_mO species as initial intermediates in the dissociation. The first is called the carbide mechanism and the second the hydrogen-assisted mechanism.[5-10] To unravel this problem we performed experiments using two complementary in *situ* x-ray techniques: EY-XAS and APXPS.

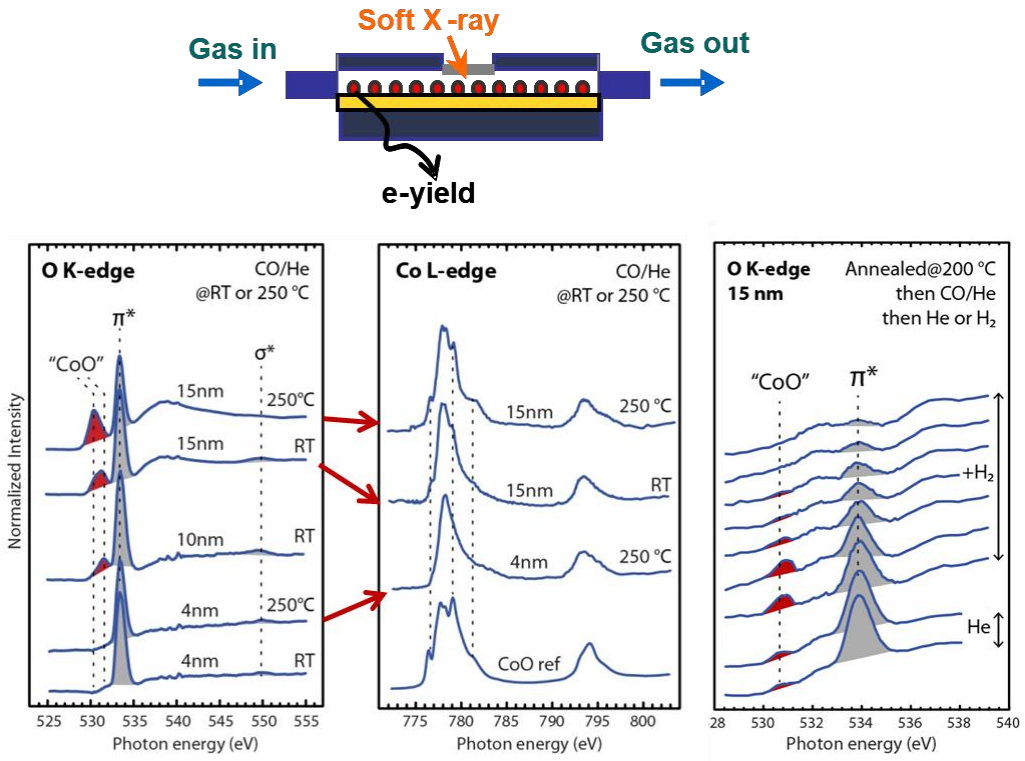

Fig. 1. Top: Schematic of the cell sealed with an x-ray transparent SiN membrane and gas circulation. The Co nanoparticles are deposited on a Au foil which serves as the collector for the EY-XAS current. Bottom left: O *K*-edge EY-XAS spectra of nanoparticles after exposure to CO/He (1:1) at r.t. and 250 °C. The peak at 534 eV corresponds to excitation to the π^* orbital of CO. The peak 531 eV (filled with red) is from CoO. Center: corresponding Co L-edge spectra showing oxidation state of Co. Right: O *K*-edge spectra of a 15 nm cobalt nanoparticle after annealing in He at 200 °C and subsequent exposure to CO/He and then H_2. Adsorbed H activates CO dissociation and later reduces CoO until all adsorbed CO is consumed. Adapted from Ref. 12. Copyright (2013) American Chemical Society.

In the ET-XAS experiment Co nanoparticles (NP) with diameters ranging from 4 to 15 nm were deposited on a gold foil substrate in a gas cell sealed with a 100 nm thick Si_3N_4 nitride window. This membrane separates the reactor volume from the vacuum chamber of the Synchrotron beamline.[11] The Co NP were cleaned by alternating cycles of oxidation and reduction with O_2 and H_2, both at 1 atm. This was followed by

adsorption of CO from a 1:1 mixture of CO and He at one atmosphere. After this the CO was removed from the gas phase and EY-XAS data acquired in pure He. The spectra revealed the presence of molecularly adsorbed CO, as detected by the π^* resonance in the O K-edge EY-XAS, (Fig. 1a). Introduction of H_2 (1 atm). resulted in the rapid dissociation of CO, which produced CoO. The oxide was reduced by H_2 until all adsorbed CO was consumed. Interestingly, even small amounts of hydrogen, chemisorbed on the Co from the initial reducing treatment, or from background H_2, led to some build-up of CoO from CO dissociation, indicating the high reactivity of CO to H, even at room temperature.[12]

These results were verified by APXPS using Co foils, although in that case the pressure was substantially lower, in the 0.1-1 Torr range. The APXPS chamber in Beamline 11.0.2 of the Advanced Light Source (the Berkeley Synchrotron Facility), could be pumped to initial background pressures in the 10^{-10} Torr range. The use of a Co foil instead of nanoclusters made possible to clean the sample using surface science methods of Ar ions sputtering and annealing, as well as providing a better control the initial background pressure of residual gases, particularly H_2. After such cleaning the Co foil exhibited some residual C in the form of carbide (CoCx) and adventitious carbon from contamination (CH_x). The sample was then exposed to 0.5 Torr of CO, which saturated the surface and protected it from contamination by background gases. After evacuation of the CO gas phase some of the surface bound CO desorbed at RT, leaving about one third of the initial coverage. This produced the spectrum shown on the left graph of Fig.2a (top, blue), showing the C XPS peak from CO and from residual carbide. By heating the sample in vacuum to increasing temperatures all the CO desorbed, with only a small increase in the carbide peak, likely from residual H contamination (Fig. 2b). This demonstrates that the desorption rate of CO molecules is higher than the dissociation rate to C and O. It is possible to dissociate CO in the absence of H, but the process requires a higher temperature. This “direct” dissociation could be observed only when a sufficiently high pressure of CO was maintained while during heating. As shown in Fig. 2c,d, under 0.1 Torr of CO dissociation produces a rapid increase of Co carbide (and Co oxide, not shown here) above 100 ^{o}C. At this temperature in vacuum all CO had desorbed already. The oxide is subsequently reduced in the presence of CO to form CO_2 gas.

When H_2 was introduced to total pressure of 0.1 Torr with three different CO:H_2 ratios of 97: 3, 9:1, and 1:1, a rapid increase in the coverage of CoO was observed already a room temperature, indicative of the efficient dissociation of CO by reaction with adsorbed H.[13]

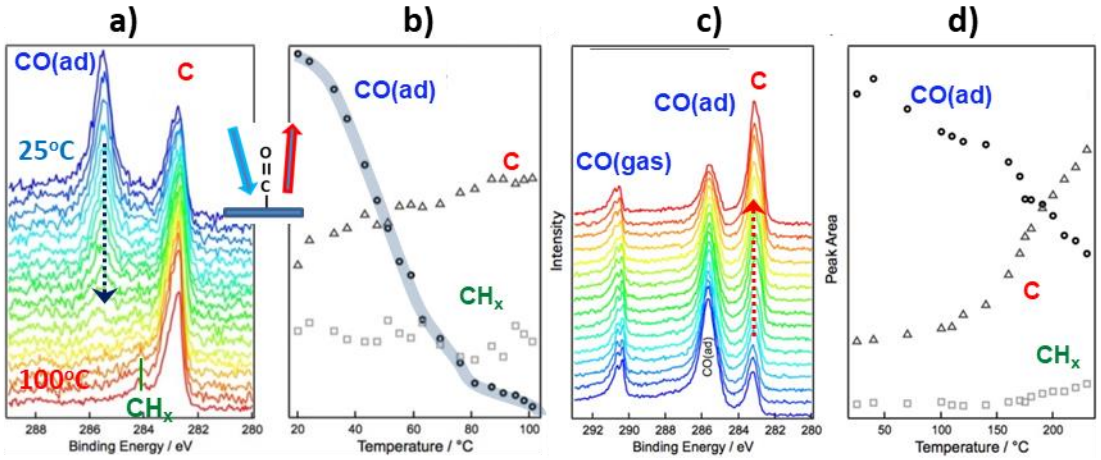

Fig. 2. APXPS showing the CO desorption and decomposition on a cobalt foil. a) C*1s* spectra acquired in UHV after pre-adsorbing CO. The spectra colors, from blue to red, correspond to increasing temperatures from RT to 100°C; b) Peak areas of adsorbed CO (CO(ad)), carbide (C), and hydrocarbon contaminants (CH_x) as a function of temperature, from areas of peak fittings in a); c) APXPS showing the thermally induced CO dissociation under 100 mTorr CO. The colors, from blue to red, correspond to temperatures from RT to 230°C; d) Peak areas of adsorbed CO, carbide, and contamination as a function of temperature. Because of the lower activation energy for desorption, dissociation can only be observed by maintaining CO in the gas phase. In both cases the x-ray photon energy E_{hv} = 490 eV. Adapted from Ref. [13]. Copyright (2017) American Chemical Society.

Ambient pressure STM and APXPS reveal how the reconstruction of catalysts by adsorbates

The following example illustrates an important aspect of the pressure gap. This is the "kinetic gap", or quenching of metastable structures due to low kinetics in UHV, while at room temperature and above this limitation is not present. This is particularly notable in experiments where coverage of weakly adsorbed reactants can only be obtained at cryogenic temperatures in UHV, while at RT a sufficiently high pressure serves to stabilize steady-state coverage in equilibrium with the gas. In the following example we show the unexpected changes that occur a single crystal Cu catalyst exposed to CO at room temperature.[14] Copper is an active catalyst in the important water-gas shift

reaction. Since CO binds weakly to Cu (0.47 eV on the (111) surface), temperatures below 200K are necessary to produce a stable coverage of molecules for surface science experiments.

Figure 3 shows STM images of the Cu(111) surface first in UHV at RT (left top image), where the sample can be seen as consisting of large terraces, 10 to 100 nm wide, separated by monoatomic steps. Upon exposure to CO the surface remained unchanged for pressures below 10 mTorr, but changed dramatically when the pressure reached 100 mTorr and higher (left, middle image). The terraces filled with clusters of Cu atoms with shapes roughly hexagonal, although changing continuously with time. The edges of these clusters are decorated by CO molecules, visible in the images as bright protrusions. This was explained as follows: CO adsorbs on the surface preferentially at low coordinated Cu atoms such as those in step edges, where its binding energy is about 0.77 eV, i.e., 0.3 eV higher than on the flat terraces. The CO has two effects: one it causes a weakening of the Cu-Cu binding of the atoms it bounds to, such that they can more easily detach and reassemble into clusters; second it lowers the Cu diffuse barrier when bound to a CO molecule. Using the area of C and O peaks in APXPS and the length of step and cluster edges measured in STM images, such as that in Fig.3 (left middle), we could determine that in equilibrium the gas, the amount of adsorbed CO molecules is equivalent to the number of edge atoms. Increasing the CO pressure caused formation of more clusters to accommodate additional molecules. This process continues until the number of clusters fills completely the surface, which occurs at about 10 Torr at RT. Interestingly, upon removal of the gas phase all the CO molecules desorb, leaving a roughened surface due to the slower kinetics of Cu diffusion, such that heating was necessary to restore the original flat structure.

The new ‘clusterized’ surface was found to be much more active catalyzing water dissociation, a crucial step in the WGS reaction: $CO+H_2O \leftrightarrow CO_2+H_2$. Indeed, molecular water does not adsorb on the pristine flat Cu(111) surface at room temperature (Fig 3, top right XPS), but adsorbs dissociatively on the more active Cu(110) surface [15]. When the ‘clusterized’ Cu(111) surface was exposed to 2×10^{-9} Torr of H_2O (after CO desorption), water dissociated readily as shown by APXPS (Fig. 3 bottom right). [14]

This example illustrates the capital important of determining the structure of surfaces under high pressures, and how new structures can be formed that have catalytic properties that can be very different those of the pristine model surfaces prepared in UHV conditions. A similar behavior was observed for other Cu surface orientations. [16,17]

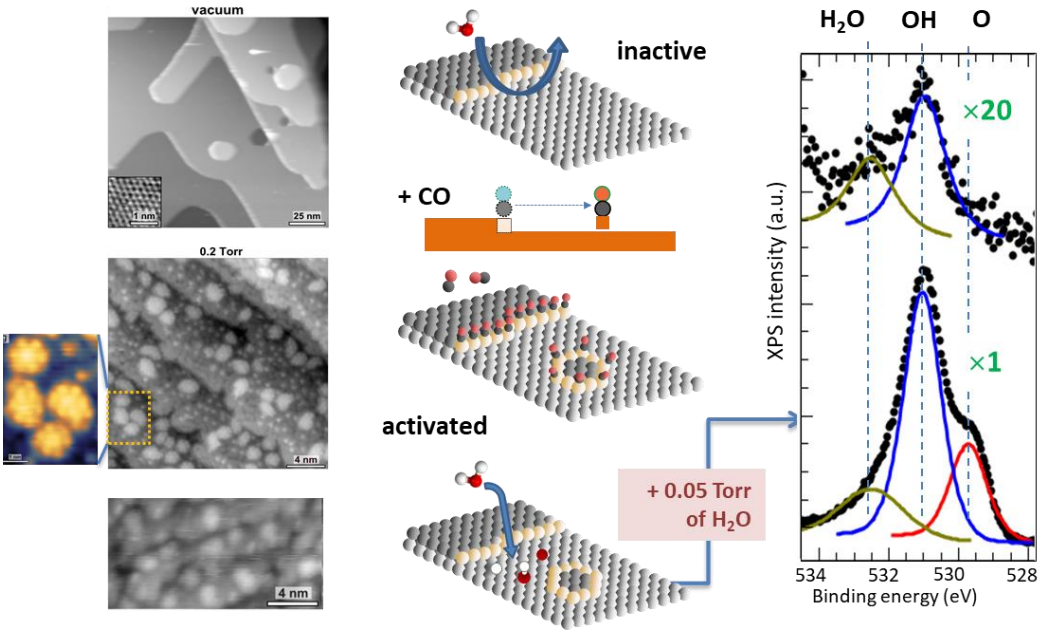

Figure 3. STM images of Cu(111) as a function of ambient CO pressure. Left: In UHV. The inset shows atomically resolved Cu atoms in the terrace. Center: under 0.2 Torr of CO, many clusters form on the terraces. Right: expanded images of two types of hexagonal clusters of 19 Cu atoms with C_6 or C_3 symmetry, shown colored in the center image. Adapted from ref. 14. Copyright © 2016, AAAS

Extending the pressure range by using x-ray and electron transparent membranes

The above two examples offer a glimpse of the new understanding of surfaces and the new phenomena that emerge from the application of the new *in situ/operando* spectroscopy and microscopy techniques, developed over the last decades. Now we briefly show some new possible avenues to further extend the pressure range not only into the atmospheric range, but also to include interfaces between surfaces and condensed phases such as liquids, of capital importance in electrochemical processes, photo- and electro-catalysis, batteries, and more. One obvious way to extend the pressure range is by reducing the travel distance between excited electrons and the analyzer. In APXPS this implies reducing the sample-analyzer distance, working with smaller entrance apertures,

and of course with better electron optics and differential pumping. This is an active area of development pursued both in commercial and laboratory instruments. Higher pressures can also be achieved using x-rays of higher energy to decrease the scattering cross section of the more energetic photoelectrons. We will not cover this topic here however.

In a different approach, thin (~100 nm) Si_3N_4 membranes have been used to seal small cells that filled with gases or liquids at ambient atmospheric pressure. While the membranes are too thick for electrons to pass through to the analysis area in the vacuum side, they can be used for XAS experiments in fluorescence and electron yield modes, as in the example shown above for Co NP catalysts. Another recent example using Si_3N_4 membranes is a study of solid-liquid interfaces with EY-XAFS. The sample in this case is the working electrode deposited as a thin film (~20 nm) on the back side of the Si_3N_4 membrane sealing a small electrochemical cell. The sample has two roles, one is as electrode and the other as collector of the secondary electrons generated by the decay of the core holes of species near the electrode-solution interface. The short mean free path of electrons in condensed matter provides the interface sensitivity of the method. The first example was a study of the H-boding structure and orientation of water molecules near a gold electrode and the effect of the electric field in the double layer. We will not cover is this short review this very promising method but refer the reader to the first publication on the topic. [18]

Restricting our discussion to XPS, an emerging new methods is to use electron transparent membranes, such as graphene, boron nitride, and possibly other layered materials, which are strong enough to support pressure differentials of one or several atmospheres graphene and also transparent to moderate energy electrons, which makes them ideal for atmospheric pressure surface studies. [19- 21]

In our laboratory we deposited the graphene on a 100 nm thick holy Si_3N_4, as shown in Figure 4.[22] The purpose of the holes is twofold: to provide mechanical support, and to limit the area of suspended graphene to one micrometer approximately. This is necessary because current methods of graphene production by chemical vapor deposition (CVD) on Cu foil produce many defects, grain boundaries, etc. that cause graphene to be chemically unstable and easy to rupture. Since typical grain sizes of the CVD graphene are in the micrometer range, holy Si_3N_4 substrate greatly alleviates the problems mentioned. In our laboratory, graphene chemically detached from the Cu substrate was deposited on holy a Si_3N_4 window. Previous to deposition the Si_3N_4 was covered with a thin layer of Au (other metals work also), about a few ten nm thick, to improve adherence and to ensure electrical continuity of the graphene layer. Figure 4 shows an SEM image

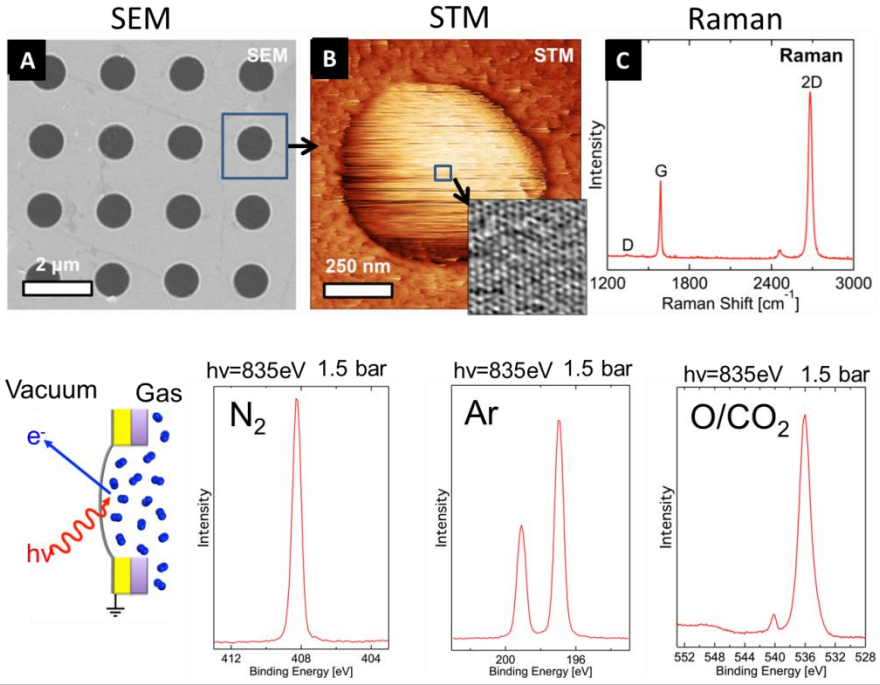

Fig. 4 . Top: A) SEM image of a holy SiN membrane (1 um diameter) covered by a single layer graphene (SLG). B) STM image of one the holes in the membrane with SLG suspended across it. The inset shows an atomic resolution STM image of free-standing graphene. C) Raman spectra of SLG transferred onto SiO_2(300 nm)/Si using the same method used for fabricating the graphene-based membranes. Bottom: Schematic of the XPS experiment, showing one of the holes and the SLG separating vacuum in the Synchrotron beam line on the left and gas on the right inside the cell. The pressure can reach up to 2.5 bar (~atm), depending on the quality and defects of the graphene. Three spectra are shown for N2, Ar and CO2 on the right at 1.5 bar. Other gases are also possible (H_2, He, CO). The OK-level peak in CO2 shows two peaks, on from the CO2 gas molecules, the other at 540 eV from O bound to the graphene due to beam damage. Adapted from Ref. [22]. Copyright (2017) American Chemical Society.

of the holy Si_3N_4 covered with graphene (1 um holes), and an STM image of an area near the top of the suspended graphene.

With such graphene covered cells XPS from several gases, like H_2, He, Ar, N_2, O_2, CO, CO_2 were obtained at pressures well above one atmosphere (~1 Bar), as shown in Fig. 4 for N_2, Ar and O from CO_2.

While not yet completely controlled, the use of such membrane methods is promising for extending the range of pressures where XPS studies can be pursued, for example on metal clusters deposited on the graphene membrane. Even liquids can be studied using graphene layer membranes as shown recently.[23] As we discuss in the next section however, these methods are still in their infancy and many problems and difficulties remain that need to be solved before they can be reliably utilized.

Experimental challenges in ambient pressure surface science: vacuum issues and damage by ionizing radiation

As we have seen, the techniques described above bring a plethora of new information and understanding on the structure of surfaces exposed to gases and liquids at ambient pressure and temperatures. They bring also new problems that need to be understood and addressed when studying surfaces under such conditions. The need becomes more urgent by the increasing popularization of the techniques and methods discussed above. We will discuss two of these problems here.

One trivial but sometimes overlooked problem is contamination from background gases. This is because of the difficulty of creating a gas environment in the Torr and higher pressure range where contaminants have partial pressures in the 10^{-9} Torr range. As is well known from UHV surface science, this is necessary to keep surfaces clean for times allowing for experiments to be completed i.e., one hour typically. A quick calculation reveals that if the gases introduced into a reaction chamber were to adsorb and displace a monolayer of molecules from the chamber walls (H, CO, CO_2, hydrocarbons, etc.) the partial pressure of the released molecules would be of the order of 1m Torr. This indicates the importance of carefully out-gassing the chamber by thorough bake-out procedures. A particularly simple and useful method is to strip the walls of adsorbates by igniting a plasma of N_2 or other gases prior to bake-out. Contamination from background

gases displaced from walls can be a more acute problem in public access facilities such as Synchrotron sources, where various users share the same chamber. This requires sometimes a few days of cleaning.

Perhaps the more difficult issues arise from radiation beam damage effects, directly on the samples, or indirectly by radicals created at ambient pressures from the gases illuminated by x-rays. These issues are known and have been extensively investigated in the past. Unfortunately they are not given sufficient attention because their evaluation requires sacrificing precious "beam time" in a facility to determine and to control the effects. Organic molecules are particularly prone to damage by x-rays, and even more so by the secondary electrons produced in the sample. An example that illustrates this is the degradation of alkylthiols on Au studied in the author's laboratory. In approximately 10 sec, damage reached 40% of the total in an undulator beamline at the Advanced Light Source Synchrotron in Berkeley. Lowering the x-ray intensity by about 1000 times and defocusing (in a bending magnet beamline), increased the time to reach similar degradation to a more manageable 30 minutes [24]. Another effective way to reduce beam damage is to displace the x-ray spot on the sample after short periods [24].

Inorganic materials are also susceptible to beam damage. For example loss of one component in binary systems, usually anions, can be severe in ionic crystals [25]. X-rays were observed to cause oxidation of Au in the presence of 1 Torr of O_2 due to creation of radicals, and in the same experiment the oxide was reduced to metallic Au by x-ray illumination once the O_2 gas was evacuated [26].

Liquids and condensed phases can be even more susceptible to damage from radiolysis of the liquid. For example X-ray absorption measurements of metal films in aqueous alkali halide solutions revealed changes in the oxidation state of the metal. However the extent of damage varied depending on the system. While it was severe for Cu in NaOH (0.1 M), for Ni films in $NaHCO_3$ solutions the oxidation state of the surface was stable under X-ray illumination and could be electrochemically cycled between reduced and oxidized states.[27] Some solutions to this problem include rapid circulation of the liquid in the cells so that the radiolysis products are rapidly removed from the vicinity of the active electrodes, by efficient liquid circulation of by stirring, both easily feasible, although not always implemented in user facilities.

In spite of these problems, we are optimistic that with a thorough understanding of the origin of damage, more efficient and sensitive detectors, more precise and fast displacement of the sample, and other procedures like those pointed here, will be developed to minimize damage to workable levels.

Acknowledgments

This work was supported by the Office of Basic Energy Sciences (BES), Division of Materials Sciences and Engineering, of the U.S. Department of Energy (DOE) under Contract No. DE-AC02-05CH11231, through the Structure and Dynamics of Materials Interfaces (FWP KC31SM).

References

[1] C. R. Brundle, Charles A. Evans, and Shaun Wilson. Encyclopedia of Materials Characterization: Surfaces, Interfaces, Thin Films. Butterworth-Heinemann, 1992

[2] Clare E. Harvey and Bert M. Weckhuysen. Surface- and Tip-Enhanced Raman Spectroscopy as Operando Probes for Monitoring and Understanding Heterogeneous Catalysis. Catal Letters 2015; 145(1): 40–57.

[3] D. Frank Ogletree, H. Bluhm, G. Lebedev, C. Fadley, Z. ssaiHun and M. Salmeron. A differentially pumped electrostatic lens system for photoemission studies in the millibar range. Rev. Sci. Instr. 73, (11) 3872-3877 (2002)

[4] M. Salmeron and R. Schlögl. Ambient pressure photoelectron spectroscopy: A new tool for surface science and nanotechnology. Surf. Sci. Rep. 63, 169 (2008).

[5] Schulz, H. Short history and present trends of Fischer–Tropsch synthesis. Appl. Catal., A 1999, 186, 3.

[6] Bell, A. T. Catalytic Synthesis of Hydrocarbons over Group VIII Metals. A Discussion of the Reaction Mechanism. Catal. Rev. 1981, 23, 203.

[7] Shetty, S.; Jansen, A. P. J.; van Santen, R. A. Direct versus Hydrogen-Assisted CO Dissociation. J. Am. Chem. Soc. 2009, 131, 12874.

[8] van Helden, P.; van den Berg, J. A.; Ciobica, I. M. Hydrogen assisted CO dissociation on the Co (211) stepped surface. Catal. Sci.Technol. 2012, 2, 491.

[9] Blyholder, G.; Lawless, M. Hydrogen-Assisted Dissociation of CO on a Catalyst Surface. Langmuir 1991, 7, 140.

[10] Inderwildi, O. R.; Jenkins, S. J.; King, D. A. Fischer−Tropsch Mechanism Revisited: Alternative Pathways for the Production of Higher Hydrocarbons from Synthesis Gas. J. Phys. Chem. C 2008, 112, 1305.

[11] Escudero, C.; Jiang, P.; Pach, E.; Borondics, F.; West, M. W.; Tuxen, A.; Chintapalli, M.; Carenco, S.; Guo, J.; Salmeron, M., A reaction cell with sample laser heating for in situ soft X-ray absorption spectroscopy studies under environmental conditions. J. Synchrotron Radiat. 2013, 20 (3), 504-508.

[12] Tuxen, A.; Carenco, S.; Chintapalli, M.; Chuang, C.-H.; Escudero, C.; Pach, E.; Jiang, P.; Borondics, F.; Beberwyck, B.; Alivisatos, A. P.; Thornton, G.; Pong, W.-F.;

Guo, J.; Perez, R.; Besenbacher, F.; Salmeron, M., Size-Dependent Dissociation of Carbon Monoxide on Cobalt Nanoparticles. *J. Am. Chem. Soc.* **2013,** *135* (6), 2273-2278

[13] Wu, C.H.; Eren, B.; Bluhm, H.; Salmeron, M. B., Ambient-Pressure X-ray Photoelectron Spectroscopy Study of Cobalt Foil Model Catalyst under CO, H_2, and Their Mixtures. ACS *Catal.* **2017,** *7* (2), 1150-1157

[14] Eren, B.; Zherebetskyy, D.; Patera, L. L.; Wu, C. H.; Bluhm, H.; Africh, C.; Wang, L.-W.; Somorjai, G. A.; Salmeron, M., Activation of Cu(111) surface by decomposition into nanoclusters driven by CO adsorption. *Science* **2016**, 351, 475-478.

[15] S. Yamamoto, K. Andersson, H. Bluhm, G. Ketteler, D. E. Starr, T. Schiros, H. Ogasawara, L. G. M. Pettersson, M. Salmeron, A. Nilsson, Hydroxyl-Induced Wetting of Metals by Water at Near-Ambient Conditions, J. Phys. Chem. C 111, 7848–7850 (2007).

[16] Eren, B.; Zherebetskyy, D.; Hao, Y.; Patera, L. L.; Wang, L.-W.; Somorjai, G. A.; Salmeron, M., One-dimensional nanoclustering of the Cu(100) surface under CO gas in the mbar pressure range. *Surf. Sci.* **2016**, 651, 210-214.

[17] Eren, B.; Liu, Z.; Stacchiola, D.; Somorjai, G. A.; Salmeron, M., Structural Changes of Cu(110) and Cu(110)-(2 × 1)-O Surfaces under Carbon Monoxide in the Torr Pressure Range Studied with Scanning Tunneling Microscopy and Infrared Reflection Absorption Spectroscopy. *J. Phys. Chem. C* **2016,** *120* (15), 8227-8231

[18] . J. J. Velasco-Velez, C. H. Wu, Tod A. Pascal, L. F. Wan, J.-H. Guo, David Prendergast, and Miquel B. Salmeron. The structure of interfacial water on gold electrodes studied by x-ray absorption spectroscopyScience. 346, 831-834 (2014).

[19] Krueger, M.; Berg, S.; Stone, D.; Strelcov, E.; Dikin, D. A.; Kim, J.; Cote, L. J.; Huang, J.; Kolmakov, A. Drop-Casted Self-Assembling Graphene Oxide Membranes for Scanning Electron Microscopy on Wet and Dense Gaseous Samples. ACS Nano 2011, 5, 10047−10054.

[20] Yuk, J. M.; Park, J.; Ercius, P.; Kim, K.; Hellebusch, D. J.; Crommie, M. F.; Lee, J. Y.; Zettl, A.; Alivisatos, A. P. High-Resolution EM of Colloidal Nanocrystal Growth Using Graphene Liquid Cells. Science 2012, 336, 61−64.

[21] Kolmakov, A.; Dikin, D. A.; Cote, L. J.; Huang, J.; Abyaneh, M. K.; Amati, M.; Gregoratti, L.; Günther, S.; Kiskinova, M. Graphene Oxide Windows for in Situ Environmental Cell Photoelectron Spectroscopy. Nat. Nanotechnol. 2011, 6, 651−657.

[22] Weatherup, R. S.; Eren, B.; Hao, Y.; Bluhm, H.; Salmeron, M. B., Graphene Membranes for Atmospheric Pressure Photoelectron Spectroscopy. *J. Phys. Chem. Lett.* **2016,** *7* (9), 1622-1627.

[23] Velasco-Velez, J. J.; Pfeifer, V.; Haevecker, M.; Weatherup, R. S.; Arrigo, R.; Chuang, C.-H.; Stotz, E.; Weinberg, G.; Salmeron, M.; Schloegl, R.; Knop-Gericke, A., Photoelectron Spectroscopy at the Graphene-Liquid Interface Reveals the Electronic Structure of an Electrodeposited Cobalt/Graphene Electrocatalyst. *Angew. Chem., Int. Ed.* **2015,** *54* (48), 14554-14558

[24] G Ketteler, P Ashby, B.S. Mun, I. Ratera, H. Bluhm, B. Kasemo, and M. Salmeron. In situ photoelectron spectroscopy study of water adsorption on model biomaterial surfaces. G Ketteler, P Ashby, B.S. Mun, I. Ratera, H. Bluhm, B. Kasemo, and M. Salmeron. J. Phys.: Condens. Matter. 20, 184024 (2008).

[25] Kenta Arima, Peng Jiang, Xingyi Deng, Hendrik Bluhm, Miquel Salmeron. Water Adsorption, Solvation, and Deliquescence of Potassium Bromide Thin Films on SiO_2 Studied by Ambient-Pressure X-ray Photoelectron Spectroscopy. J. Phys. Chem. C. 114, (35), 14900–14906 (2010).

[26] Peng Jiang, Soeren Porsgaard, Ferenc Borondics, Mariana Köber, Alfonso Caballero, Hendrik Bluhm, Flemming Besenbacher, Miquel Salmeron. Room-Temperature Reaction of Oxygen with Gold: An In situ Ambient-Pressure X-ray Photoelectron Spectroscopy Investigation. J. Am. Chem. Soc. 132, 2858–2859 (2010).

[27] Robert S. Weatherup, Cheng Hao Wu, Carlos Escudero, Virginia Pérez-Dieste, Miquel B. Salmeron. Environment-Dependent Radiation Damage in Atmospheric Pressure X-ray Spectroscopy. J. Phys. Chem. B. (2017). DOI:10.1021/acs.jpcb.7b06397